

# **Incorporation of Reaction Kinetics into a Multiphase, Hydrodynamic Model of a Fischer Tropsch Slurry Bubble Column Reactor**

**2008 AIChE Annual Meeting**

Donna Post Guillen  
Anastasia M. Gribik  
Jonathan K. Shelley  
Steven P. Antal

**November 2008**

This is a preprint of a paper intended for publication in a journal or proceedings. Since changes may be made before publication, this preprint should not be cited or reproduced without permission of the author. This document was prepared as an account of work sponsored by an agency of the United States Government. Neither the United States Government nor any agency thereof, or any of their employees, makes any warranty, expressed or implied, or assumes any legal liability or responsibility for any third party's use, or the results of such use, of any information, apparatus, product or process disclosed in this report, or represents that its use by such third party would not infringe privately owned rights. The views expressed in this paper are not necessarily those of the United States Government or the sponsoring agency.

The INL is a  
U.S. Department of Energy  
National Laboratory  
operated by  
Battelle Energy Alliance



## INCORPORATION OF REACTION KINETICS INTO A MULTIPHASE, HYDRODYNAMIC MODEL OF A FISCHER TROPSCH SLURRY BUBBLE COLUMN REACTOR

Donna Post Guillen, Anastasia M. Gribik, and Jonathan K. Shelley  
Donna.Guillen@inl.gov, Anastasia.Gribik@inl.gov, Jonathan.Shelley@inl.gov  
Idaho National Laboratory  
PO Box 1625  
Idaho Falls, ID 83415-3710, USA

Steven P. Antal  
antals@rpi.edu  
Department of Mechanical, Aerospace, and Nuclear Engineering  
Rensselaer Polytechnic Institute  
110 8th Street  
Troy, NY 12180-3590, USA

### ABSTRACT

This paper describes the development of a computational multiphase fluid dynamics (CMFD) model of the Fischer Tropsch (FT) process in a Slurry Bubble Column Reactor (SBCR). The CMFD model is fundamentally based which allows it to be applied to different industrial processes and reactor geometries. The NPHASE CMFD solver [1] is used as the robust computational platform. Results from the CMFD model include gas distribution, species concentration profiles, and local temperatures within the SBCR. This type of model can provide valuable information for process design, operations and troubleshooting of FT plants. An ensemble-averaged, turbulent, multi-fluid solution algorithm for the multiphase, reacting flow with heat transfer was employed. Mechanistic models applicable to churn turbulent flow have been developed to provide a fundamentally based closure set for the equations. In this four-field model formulation, two of the fields are used to track the gas phase (i.e., small spherical and large slug/cap bubbles), and the other two fields are used for the liquid and catalyst particles. Reaction kinetics for a cobalt catalyst is based upon values reported in the published literature. An initial, reaction kinetics model has been developed and exercised to demonstrate viability of the overall solution scheme. The model will continue to be developed with improved physics added in stages.

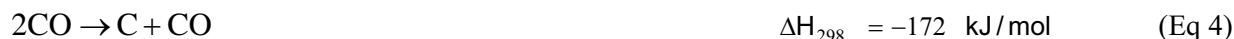
### INTRODUCTION

As part of the Idaho National Laboratory's (INL's) Secure Energy Initiative, the INL is performing research in areas that are vital to ensuring clean, secure energy for the nation. Specifically, our team is developing a computational multiphase fluid dynamics (CMFD) model of Fischer Tropsch (FT) synthesis in a slurry bubble column reactor (SBCR) used for the production of synthetic fuels from secure, domestic resources. The model is being developed using a staged approach, starting with a simple model then becoming progressively more complex. Reaction kinetics have been incorporated into a hydrodynamic model for churn-turbulent flow using the NPHASE CMFD code as the robust numerical solver [1, 2]. The purpose of this model is to help industry understand the complex physical processes occurring in the SBCR. The model can be used as a numerical testbed to study custom problems that concern industry and gain a better understanding of the mechanisms that govern reactor performance from a more fundamental perspective than has been done in the past. To date, much of the understanding of these types of reactors has been obtained by limited studies using correlations that are not widely applicable over a range of operating conditions and scales. A more fundamental, mechanistic-based model that is broadly applicable is needed to enable efficient reactor design studies and scaling over the range from laboratory to pilot reactors and finally commercial production scales. To make the process economically viable, the designer must optimize reactor performance by varying operating conditions eliminating dead zones within the reactor. An understanding of the mixing behavior is essential for proper

design and scale-up [3]. Simulations can be used to locate regions of maximum and minimum velocity and temperature, to facilitate identification of these dead zones and/or regions of excessively high temperatures, as well as predict any mass or heat transfer design limitations for the reactor. More sophisticated physicochemical models offer the potential to bring an increased level of understanding for the basic reaction and transport processes occurring within the reactor, with the eventual goal of being able to simulate the entire FT process and the associated plant [4]. Such knowledge will enable advances in process technology that are necessary for companies to remain world-class and competitive by enabling higher productivity, reducing pollution, using less energy and resources, and improving product quality.

## REACTION KINETICS AND HYDRODYNAMICS MODEL DEVELOPMENT

An NPHASE CMFD model of the FT process in a SBCR is under development. The SBCR is a multiphase chemical reactor where a synthesis gas, comprised mainly of H<sub>2</sub> and CO, is bubbled through a liquid hydrocarbon wax containing solid catalyst particles to produce specialty chemicals, lubricants, or liquid fuels. The FT synthesis reaction is the polymerization of methylene groups  $[-(\text{CH}_2)-]$  forming mainly linear alkanes and alkenes, ranging from methane to high molecular weight waxes. The FT process is described by the set of exothermic reactions described by Eqs 1-4



The selection of catalyst (i.e., avoiding Ni) can minimize the production of methane, the reaction shown in Eq 1. The chain polymerization kinetics in Eq 2 produces a hydrocarbon product distribution described by the Anderson-Schulz-Flory (ASF) model. A broad spectrum of mainly alkanes and alkenes with carbon numbers from C<sub>1</sub> to C<sub>50+</sub> are produced. Process conditions and/or catalyst selection can be used to tailor the product distribution [5]. Eq 3, the water-gas-shift (WGS) reaction, is invoked only for reactions involving Fe-based catalysts. Eq 4 is the Boudouard reaction resulting in the deposition of carbon and the formation of carbon dioxide.

The computational platform for this work is the NPHASE computer program, an unstructured, finite volume, multifield, pressure based computational multiphase fluid dynamics (CFD) computer code offering both segregated and coupled numerical solution methods. To achieve numerical convergence for multiphase flows, simulations are performed using the robust, coupled algorithm, which solves for the phasic velocity, pressure, and volume fraction simultaneously. Although, the computer memory requirements are increased, this ability to couple the conservation of mass and momentum equations is more robust than the use of a segregated solver. A full three-dimensional, Eulerian-Eulerian framework is employed, rather than tracking a very large number of individual bubble trajectories. Ensemble-averaged conservation equations for mass, momentum, energy, interfacial area, and species transport are solved for an arbitrary number of fields or phases and species. The equations are discretized into a block matrix system, which is solved by an algebraic multigrid solver. The fully coupled mass/momentum setup allows any field/phase to interact with any other field/phase within the multigrid matrix system. A detailed derivation of the ensemble-averaged conservation equations has been given by [6]. The ensemble-averaging approach models a time-varying complex multiphase flow using a well-defined theoretical

framework. The option for invoking an additional transport equation that is solved for the interfacial area concentration [7] is available in the NPHASE code and may be included in the FT model to better predict the available reaction area between the gas and bulk fluid. Interfacial mass, momentum, turbulence and heat transfer sub-models provide coupling between the fields and phases. NPHASE also includes transport equations for turbulence modeling and an arbitrary number of species in any carrier field. Turbulence in the bulk fluid was modeled using a standard  $k$ - $\epsilon$  model with the two-phase turbulence viscosity given by [8]. The total kinematic viscosity for the bulk flow is the sum of molecular, shear-induced and bubble-induced components.

In an industrial FT process, syngas is sparged at the base of a large cylindrical vessel containing liquid and catalyst. Momentum is imparted to the bulk liquid via the kinetic energy of the sparged syngas and the recirculating internal flow is driven by interfacial forces. For the process to be economically viable, the velocity of the gas must be sufficiently high that the reactor operates in the churn-turbulent flow regime.

A key factor for properly capturing the underlying physics of two-phase flows is the formulation of consistent mechanistic closure laws that describe the dominant mass, momentum and thermal interactions at the fluid interfaces. Closure relations are needed to reintroduce the information that was lost as a result of averaging the conservation equations. These closure laws account for the sub-scale mass and momentum transfer between the various fields and phases. The interfacial interactions between the individual fields are specified by mechanistic models for both drag and non-drag forces. The interfacial momentum transfers considered important for churn-turbulent flow in a bubble column include the interfacial drag force, the virtual mass force, the wall force, the lift force, and the turbulence dispersion force. Refinement of these mechanistic models is ongoing to ensure that they apply over a realistic range of operating conditions and scales. The closure relations include coefficients that need to be tuned to the physics of the flow regime. Optimization software (Engineous iSIGHT-FD) is being used to perform a sensitivity study by varying the ranges of the coefficients over their theoretically appropriate ranges.

The gas field is divided into a small (5 mm) bubble group and a large (50 mm) slug/cap bubble group. Each bubble group is treated as a separate field to allow different flow physics to be included via the closure models. The model also accounts for interactions between bubble groups (i.e., breakup and coalescence). Incorporation of a third bubble size ( $< 1$  mm) will also be evaluated in the model, since these very small bubbles present a large interfacial area available for the reaction process, relative to the bubble volume. Eventually multiple bubble groups, at least 5 groups, will be considered for future simulations.

Bubble dynamics play a key role in the transport phenomena and in the overall rates of reaction. The intrafield mass transfer between the small bubbles and slug/cap bubbles was formulated using coalescence and breakup models described by [9], [10] and [11]. Improved bubble fragmentation and coalescence sub-models are an area where more research is needed. Two opposing theories have been proposed regarding the roles of the large versus the small bubbles on mass transfer. One theory espouses the concept that large cap bubbles largely determine the flow pattern, whereas the small bubbles (assumed to be spherical) govern mass transfer. Another theory claims that the unstable, oscillating surface of the large bubbles create a high level of turbulence, which enhances mass transfer, whereas the small bubbles have a relatively rigid surface that inhibits mass transfer. Studies by [12] found that bubble fragmentation and coalescence were strongly influenced by the turbulence dissipation rate of the liquid phase.

This section presents the model formulation, governing equations and closure laws used to simulate the turbulent, four-field, two-phase flow for a bubble column operating in the churn-turbulent flow regime (see Figure 1). Figure 2 outlines the thermal fluid and chemistry features to be incorporated into the current NPHASE CMFD model. The SBCR model will continue to evolve and improve as the best

available physical sub-models are incorporated. The local instantaneous conservation equations are averaged and phasic volume fractions are introduced.

The phasic continuity equation is written as (field j for phase k)

$$\frac{\partial}{\partial t}(\alpha_{jk}\rho_{jk}) + \nabla \cdot (\alpha_{jk}\rho_{jk}\underline{u}_{jk}) = m_{jk}''' \quad (\text{Eq 5})$$

The phasic momentum equation is written as (field j for phase k)

$$\frac{\partial}{\partial t}(\alpha_{jk}\rho_{jk}\underline{u}_{jk}) + \nabla \cdot (\alpha_{jk}\rho_{jk}\underline{u}_{jk}\underline{u}_{jk}) = -\alpha_{jk}\nabla p_{jk} + \nabla \cdot \alpha_{jk} \begin{pmatrix} \tau_{=jk} \\ \tau_{=jk}^{\text{Re}} \end{pmatrix} + \alpha_{jk}\rho_{jk}\underline{g} + \underline{M}_{jk} + m_{jk}''\underline{u}_i \quad (\text{Eq 6})$$

The terms on the right hand side of the equation represent the pressure gradient, shear stress tensor, body force due to gravity, momentum exchange at interfaces and momentum flux due to mass transfer.

The compatibility condition included in the coupled solver equation set, is expressed as

$$\sum_{k=1}^n \alpha_k = 1 \quad (\text{Eq 7})$$

The phasic energy equation is written as

$$\frac{\partial}{\partial t}(\rho_{jk}h_{jk}) + \nabla \cdot (\rho_{jk}\underline{u}_{jk}h) = \nabla \cdot (\underline{q}_{jk}'' + \underline{q}_{jk}''') + \Delta H_i + h_c A(T_{liq} - T_w) \quad (\text{Eq 8})$$

The terms on the right hand side of the equation represent the conductive heat flux, the volumetric heat source due to the chemical reaction, and convective heat transfer to the heat exchanger, respectively. The energy equation is used to predict the change in liquid temperature due to the exothermic chemical reaction and heat exchanger. A simple heat exchanger model has been used which allows heat transfer from the liquid and represented as a constant temperature heat exchanger over the central region of the column. Future work should incorporate a more detailed model of the heat exchanger tubes within the SBCR including the pressure drop due to the presence of internals.

The physical phenomena in the SBCR occur at different time scales. Due to the thermal inertia of the reactor and its contents, the heat transfer scale is many orders of magnitude larger than the mass transfer/reaction time scale [13]. The chemical reaction rate is used to evaluate the rate of change in the mass fraction of the species. The local mass fractions of the chemical species are tracked using seven separate species transport equations. The reaction rate is used to evaluate the local heat addition to the bulk flow. The species transport equation can be written as

$$\frac{\partial}{\partial t}(\alpha_{jk}\rho_{jk}Y_s) + \nabla \cdot (\alpha_{jk}\rho_{jk}\underline{v}_{jk}Y_s) = \nabla \cdot \alpha_{jk} \begin{pmatrix} \mu_{jk} \\ \sigma_s \\ \mu_{jk}^T \\ \sigma_s^T \end{pmatrix} \nabla Y_s + S_s \quad (\text{Eq 9})$$

where  $Y_s$  is the species mass fraction and  $S_s$  is the source term containing the reaction kinetics

$$S_s = W_s \sum_{n=1}^{N_R} n_{sn} R_n \quad (\text{Eq 10})$$

Chemical reactions are being added in stages of increasing complexity. The first stage of the model tracks the mass fraction species of H<sub>2</sub> and CO in the gas phase and [-(CH<sub>2</sub>)-] in the liquid field and includes absorption of gas species from both large and small bubbles into the bulk liquid phase. The driving force for the gas across the interface into the bulk liquid will be dependent upon the interfacial species concentration in both small and large bubbles. However, because it is difficult to measure the concentration at the gas-liquid interface, coefficients for convective mass transfer across an interface for the overall driving force between the bulk concentrations in the gas and liquid phases are implemented. The product from the incorporation of absorption will be the steady state concentration profile of the absorbed gas species in the bulk liquid phase and the impact of the hydrodynamics on the concentration profile. All phases are assumed to have a constant density. The variation of gas density with temperature and pressure will be accounted for in future simulations.

In this initial model we assumed that the small catalyst particles are sufficiently small such that external and internal mass and heat transfer are not rate limiting. A macrokinetic approach using power rate laws is used, where the heterogeneous catalytic reaction is described by the following rate equations

$$-R_{CO} = \frac{a c_{CO,L} c_{H_2,L}}{(1 + b c_{CO,L})^2} \quad (\text{Eq 11})$$

$$-R_{H_2} = 2(-R_{CO}) \quad (\text{Eq 12})$$

$$R_{H_2O} = -(-R_{CO}) \quad (\text{Eq 13})$$

$$R_{-(CH_2)-} = -(-R_{CO}) \quad (\text{Eq 14})$$

with the kinetic constant  $a$  and the adsorption coefficient  $b$  defined as follows [14]

$$a = 8.852 \cdot 10^{-13} \exp \left[ 4494.41 \frac{1}{K} \left( \frac{1}{493.15} - \frac{1}{T} \right) \right] (RT)^2 \frac{m^6}{kg_{cat} s mol} \quad (\text{Eq 15})$$

$$b = 2.226 \cdot 10^{-5} \exp \left[ -8236.15 \frac{1}{K} \left( \frac{1}{493.15} - \frac{1}{T} \right) \right] RT \frac{m^3}{mol} \quad (\text{Eq 16})$$

The reaction model utilizes the macrokinetic rate expression for a cobalt catalyst developed by Yates and Satterfield. A cobalt catalyst was selected for the initial model, since the WGS reaction can be neglected. The intrinsic kinetic expression for the consumption of CO and H<sub>2</sub>, which is a Langmuir-Hinshelwood type expression, was based on data collected over a range of industrially relevant conditions. The local mass fractions of the chemical species are evaluated using species transport equations. Seven species are currently tracked in the SBCR simulation: CO reactant in small bubbles, large bubbles and bulk liquid; H<sub>2</sub> reactant in small bubbles, large bubbles and bulk liquid; and the [-(CH<sub>2</sub>)-] reaction product in the bulk liquid. Subsequent simulations will include a product representing the average properties of the liquid hydrocarbon wax mixture (C<sub>27</sub>H<sub>56</sub>) plus water. Eventually, the entire ASF product distribution will be modeled by grouping the products into light hydrocarbons, gasoline, diesel and waxes [5].

Change in moles of the reacting species, vapor-liquid equilibrium and the resulting temperature of the catalyst and fluid phases will be solved simultaneously. To simplify the model, it is initially assumed that only CO and H<sub>2</sub> are absorbed into the liquid phase and vapor liquid equilibrium can be neglected. Later,

gas species products of the reaction will be added to the adsorption model, including H<sub>2</sub>O, CH<sub>4</sub>, CO<sub>2</sub>, C<sub>2</sub>H<sub>4</sub>, C<sub>2</sub>H<sub>6</sub>, and other light gas species, as well as vapor liquid equilibrium. Solubility will be computed from correlations developed from experimental gas solubility data for n-paraffin solvents [15].

## MODEL SETUP

A constant inlet gas superficial velocity of 60 cm/s was specified uniformly over the entire bottom of the reactor vessel. The bulk liquid mass flow rate is 1.15 kg/s. The inlet gas flow was assumed to be comprised of 25% small bubbles (5 mm) and 75% large bubbles (50 mm). The inlet mass fraction was 0.7 CO and 0.3 H<sub>2</sub>. A 10% solids loading with 75 μm catalyst particles was suspended in the liquid.

A length-to-diameter ratio (L/D) of 4.5 was used for the simulation. For subsequent work, the L/D will be increased to more closely resemble an industrial reactor. A 60 x 500 grid with refined cell size near the wall, the inlet and the free surface was used to resolve the recirculating flow field expected in the SBCR.

The free surface in the gas disengagement region near the top of the column is represented as a constant pressure surface through which gas can escape, but the liquid and catalyst can not penetrate. The liquid and catalyst can flow out of the domain via one layer of nodes along the side to allow overflow to escape the reactor.

For this analysis, the convergence criteria are based upon an average root-mean-square (RMS) change in velocity, pressure and volume fraction between iterations being less than a specified tolerance. The RMS change in velocity was less than  $1.0 \times 10^{-4}$  while the pressure RMS change was less than  $1.0 \times 10^{-2}$ . These levels are low enough that further reducing the error would not change the predicted hydrodynamic profiles.

## RESULTS AND DISCUSSION

Results from the CMFD model are presented below. Color contour plots illustrating the spatial distribution of various computed quantities are illustrated in Figures 3 through 10. The volume fraction of small bubbles, large bubbles and catalyst are shown in Figure 3. The radial distribution of gas holdup is higher at the center of the column and exhibits a power-law profile as seen in experimental data by [16]. The distribution of catalyst within the SBCR impacts the efficiency of the chemical processes and thus the productivity of column as a chemical reactor. The slug/cap bubble interfacial lift force causes a lateral migration of the larger bubbles to the central region of the column. In this simulation, no lift force was applied to the small bubbles but future simulation will include an interfacial lift force. Experimental results show that the smaller bubbles move towards the wall [17] even in churn-turbulent flows. Future simulations will apply a lift force to both bubble groups. Contours of CO, H<sub>2</sub> and [-(CH<sub>2</sub>)-] concentration are shown in Figure 4. The concentration of reactants is highest in the lower portion of the SBCR, whereas the product concentration is highest at the upper portion of the SBCR. This is a result of the reactants transformed into product as the syngas travels through the reactor. Figure 5 depicts the velocity magnitude of bulk liquid, large bubbles and catalyst. Due to the small catalyst particle size, the catalyst particles track with the bulk fluid. Figure 6 provides the reaction rate for [-(CH<sub>2</sub>)-] production, the temperature rise above inlet temperature due to the addition of heat by the exothermic reactions and the static pressure. The pressure is seen to vary as the hydrostatic pressure. The middle region of the SBCR is at the lowest temperature in the column, since this is the region over which the heat exchanger was applied. Figure 7 shows the small and large bubble CO concentration, and small and large bubble H<sub>2</sub> concentration. Figure 8 shows the diffusion rate of CO from small and large bubbles into the bulk liquid. Figure 9 gives the small and large bubble H<sub>2</sub> diffusion rate into the bulk liquid. Figure 10 shows the computed bulk fluid turbulent kinetic energy and catalyst loading. The results of parametric studies

performed using the NPHASE model indicate that it is necessary to further investigate and validate turbulent dispersion in the model.

The reader is cautioned that these results are shown to demonstrate the capabilities of the NPHASE code and have not been fully validated with data. Limited validation of the hydrodynamic model has been accomplished, but the results incorporating heat transfer and reaction kinetics have not. The hydrodynamics of an air/water bubble column flow computed with the NPHASE code have been compared to experimental data for liquid velocity and gas holdup in a previous study [1]. Agreement with experimental data was good and the code predicted the major trends exhibited by the flow. It is stressed that the results must be validated with high-quality data suitable for validating a fundamentally-based CMFD code. Much existing experimental data has been obtained for use as input to lower order models (such as the one-dimensional axial dispersion model) or to develop empirical correlations. Thus, data for global parameters (overall gas fraction or pressure drop) is much more common than that for local parameters (spatial distribution of phases, phasic velocity, etc.).

Computational simulations presented here can be used in concert with experiments to enhance our understanding of the physicochemical processes occurring within a FT SBCR. Suitable data sets for validating predictions of chemically reacting flow in a bubble column are being sought. The model can be used as an effective means for designing experiments.

#### SUMMARY

A four-field, seven-species ensemble-averaged multifluid CFD model is under development to model the flow, thermal effects and chemical concentrations within a FT SBCR. The CMFD model is fundamentally based which allows it to be applied to different industrial processes and reactor geometries. The NPHASE CMFD solver is used as the robust computational platform. Results obtained include phase distribution, velocity and species concentration profiles throughout the reactor. Additional demonstration cases and a preliminary validation of the model are underway. Suitable data to validate the model under relevant conditions (pressure, temperature, etc.) are being pursued. Future work is also needed to validate the hydrodynamics predictions and extend the present simplified model to more realistic modeling assumptions and conditions.

We are working towards the goal of multiphase, science-based computational simulations that play a significant role in the design, operation and troubleshooting of FT plants. It is our goal to develop a more fundamental, mechanistic-based model that is more broadly applicable than currently available, and can scale to prototypic sizes and operating conditions. Recent advances in CMFD modeling tools coupled with the availability of massively parallel computing platforms offers the potential realization of this goal.

#### ACKNOWLEDGMENT

Funding for this work was provided by Battelle Energy Alliance, LLC under Contract No. DE-AC07-05ID14517 with the U.S. Department of Energy.



## NOMENCLATURE

ASF	Anderson-Shulz-Flory	
CFD	computational fluid dynamics	
CMFD	computational multiphase fluid dynamics	
FT	Fischer Tropsch	
INL	Idaho National Laboratory	
RMS	root-mean-square	
SBCR	slurry bubble column reactors	
WGS	water gas shift	
$a$	unitless	kinetic constant
$b$	unitless	adsorption coefficient
$c_{i,G}$	mol/m <sup>3</sup>	bulk concentration of species $i$ in the gas phase
$c_{i,L}$	mol/	bulk concentration of species $i$ in the liquid phase
$c_i^*$	mol/m <sup>3</sup>	equilibrium concentration of species $i$ in the gas phase with the liquid
$D_{L,i}$	m <sup>2</sup> /s	diffusivity for species $i$ in the liquid phase
$D_{L,ref}$	m <sup>2</sup> /s	reference diffusion coefficient in the liquid
$h$	kJ/kg	enthalpy
$h_c$	W/m <sup>2</sup> ·K	heat transfer coefficient
$\Delta H$	kJ/mol	heat of reaction
$k_L a_i$	s <sup>-1</sup> m <sup>3</sup>	overall mass transfer coefficient for species $i$
$m'''$	kg/s·m <sup>3</sup>	interphase mass transfer rate per unit volume
$M_{jk}$	N/s·m <sup>3</sup>	interphase momentum transfer rate per unit volume
$n$	unitless	carbon number
$n_{sn}$	unitless	species $s$ in reaction $n$
$p$	Pa	pressure
$q$	W/m <sup>2</sup>	heat flux
$R$	J/mol·K	gas constant
$R_{-(CH_2)-}$	mol/kg <sub>cat</sub> s	rate of production for -(CH <sub>2</sub> )-
$R_{CO}$	mol/kg <sub>cat</sub> s	rate of consumption for CO
$R_{H_2}$	mol/kg <sub>cat</sub> s	rate of consumption for H <sub>2</sub>
$R_{H_2O}$	mol/kg <sub>cat</sub> s	rate of production for H <sub>2</sub> O
$R_i$	mol/m <sup>3</sup>	rate of mass transfer for the solute (gas) into the solvent (liquid)
$S_s$	unitless	source term
$T$	K	temperature
$\underline{v}$	m/s	velocity
$Y_s$	unitless	species mass fraction
$W_s$	kg/mol	molecular weight of species $s$
$x_n$	unitless	mass fraction

$\alpha$	unitless	void fraction
$\rho$	kg/m <sup>3</sup>	density
$\mu$	kg/m·s	viscosity
$\tau$	N/m	shear stress

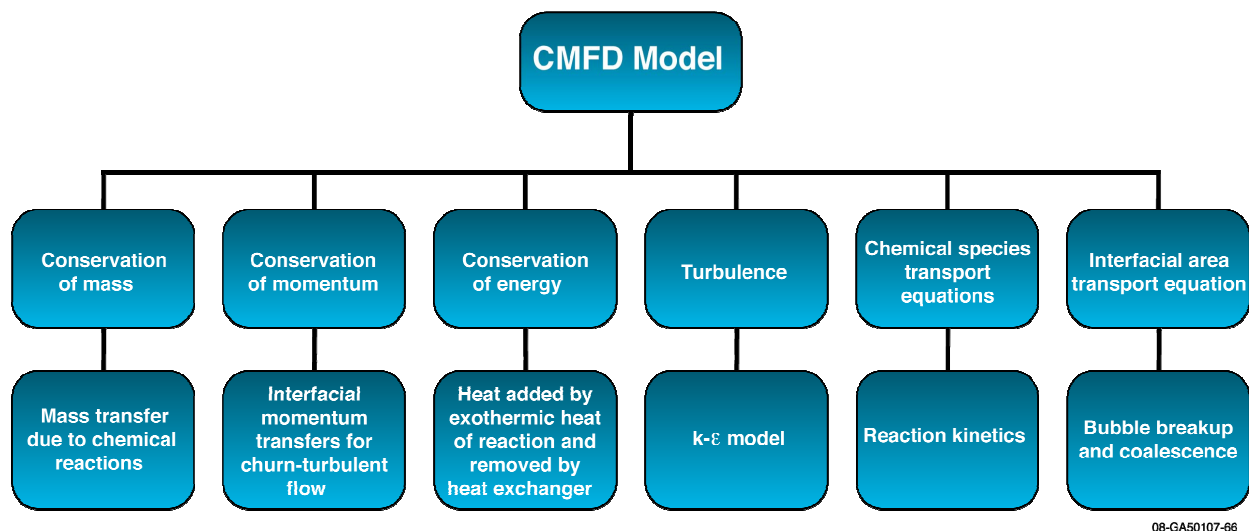
#### Subscripts

cat	catalyst
i	interfacial
j	field
k	phase
liq	liquid
w	wall

#### REFERENCES

1. Antal, S.P., R.T. Lahey, Jr., M.H. Al-Dahhan, *Simulating Churn-Turbulent Flows in a Bubble Column using a Three-Field, Two-Fluid Model*, in *5th International Conference on Multiphase Flow, ICMF'04*. 2004: Yokohama, Japan.
2. Gribik, A., Guillen, D.P., Ginosar, D., *Kinetic Modeling of a Fischer-Tropsch Reaction over a Cobalt Catalyst in a Slurry Bubble Column Reactor for Incorporation into a Computational Multiphase Fluid Dynamics Model*, in *International Pittsburgh Coal Conference 2008*. 2008, September 29 – October 2, 2008: Pittsburgh, PA.
3. Steynberg, A.P., and Dry, M.E., *Fischer-Tropsch Technology*. Studies in Surface Science and Catalysis, ed. G. Centi. Vol. 152. 2006: Elsevier.
4. Guillen, D.P., Boardman, R., Gribik, A., Wood, R., Carrington, R. *Integrated Fischer Tropsch Modular Process Model*. in *Proceedings of the 49th Annual Meeting of the Idaho Academy of Science*. 2007. Idaho Falls, ID.
5. Bartholomew, C.H., Farrauto, R.J., *Fundamentals of Industrial Catalytic Processes*. Second Edition ed. 2006, Hoboken, NJ: John Wiley & Sons, Inc. p. 402-404.
6. Drew, D.A., Passman, S.L.. "Theory of Multicomponent Fluids", *Applied Mathematical Sciences*, **Vol. 135**, (1998)
7. Murakawa, H., Antal., S.P., and Lahey, Jr., R.T. in *Proceedings of the 2008 International Congress on Advances in Nuclear Power Plants (ICAPP)*. 2008. Anaheim, CA.
8. Sato, Y., Sekoguchi, K., "Liquid Velocity Distribution in Two-Phase Bubble Flow", *Int. J. Multiphase Flow*, **Vol 2**: p. 79-95, (1975)
9. Antal, S.P., M.Z. Podowski, R.T. Lahey, Jr., D. Barber, C. Delfino, *Multidimensional Modeling of Developing Two-Phase Flows in a Large Adiabatic Riser Channel*, in *The 11th International Topical Meeting on Nuclear Reactor Thermal-Hydraulic (NURETH-11)*. 2005: Popes Palace Conference Center, Avignon, France.
10. Podowski, M.Z., Antal, S.P., Tiwari, P., Wierzbicki, B.Z., "Development of Mechanistic Models of Two-Phase Flows for the NPHASE Code," Rensselaer Polytechnic Institute, Report to the U.S. Nuclear Regulatory Commission, (2004).
11. Luo H., Svendsen, H.F., "Theoretical Model for Drop and Bubble Breakup in Turbulent Dispersions", *AIChE Journal*, **Vol. 42**, (1996)

12. Krepper, E., Lucas, D., Frank, T., Prasser, H.-M., Zwart, P.J., "The Inhomogeneous MUSIG Model for the Simulation of Polydispersed Flows", *Nuclear Engineering and Design*, **238**: p. p. 1690-1702, (2008)
13. Mahecha-Botero, A., Grace, J.R., Elnashaie, S.S.E.H., Lim, D.J., "Time-Scale Analysis of a Fluidized-Bed Catalytic Reactor Based on a Generalized Dynamic Model", *The 12th International Conference on Fluidization - New Horizons in Fluidization Engineering*, **RP4(76)**: p. p. 623-628, (2008)
14. Yates, I.C. and Satterfield, C.N., "Intrinsic Kinetics of the Fischer-Tropsch Synthesis on a Cobalt Catalyst", *Energy & Fuels*, **5**: p. 168-173, (1991)
15. Chao, K.C., Lin, H.M., "Synthesis Gas Solubility in Fischer Tropsch Slurry: Final Report," Purdue University, School of Chemical Engineering, DOE/PC/70024-T9 (1988).
16. Rados, Novica, *Slurry Bubble Column Hydrodynamics*, in *Department of Chemical Engineering*. 2003, Washington University: Saint Louis, Missouri.
17. Lucas, D., Krepper, E., Prasser, H.-M., Manera, A., "Investigations on the Stability of the Flow Characteristics in a Bubble Column", *Chem. Eng. Technol.*, **29(9)**: p. p. 1066-1072, (2006)



08-GA50107-66

Figure 1. Overview of CMFD FT model.

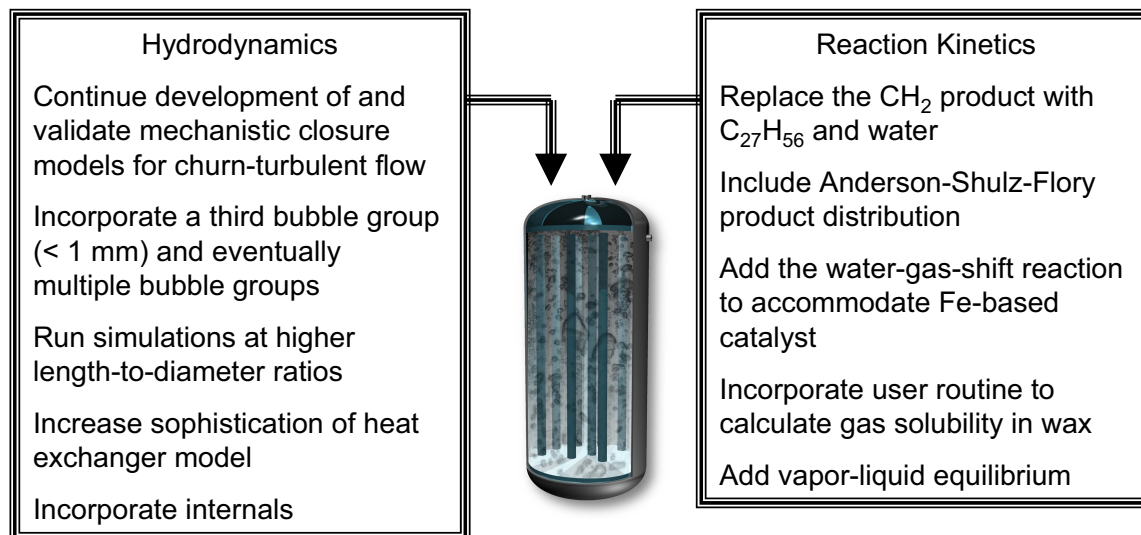


Figure 2. Staged approach to incorporating physicochemical features into preliminary model.

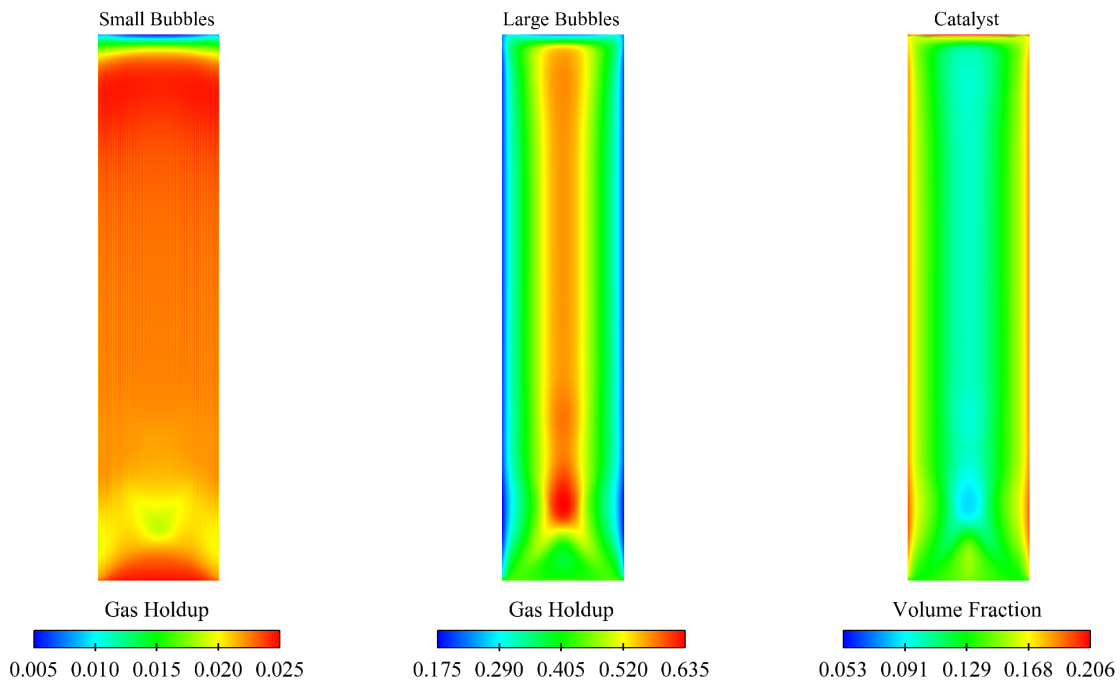


Figure 3. Volume fraction of small bubbles, large bubbles and catalyst.

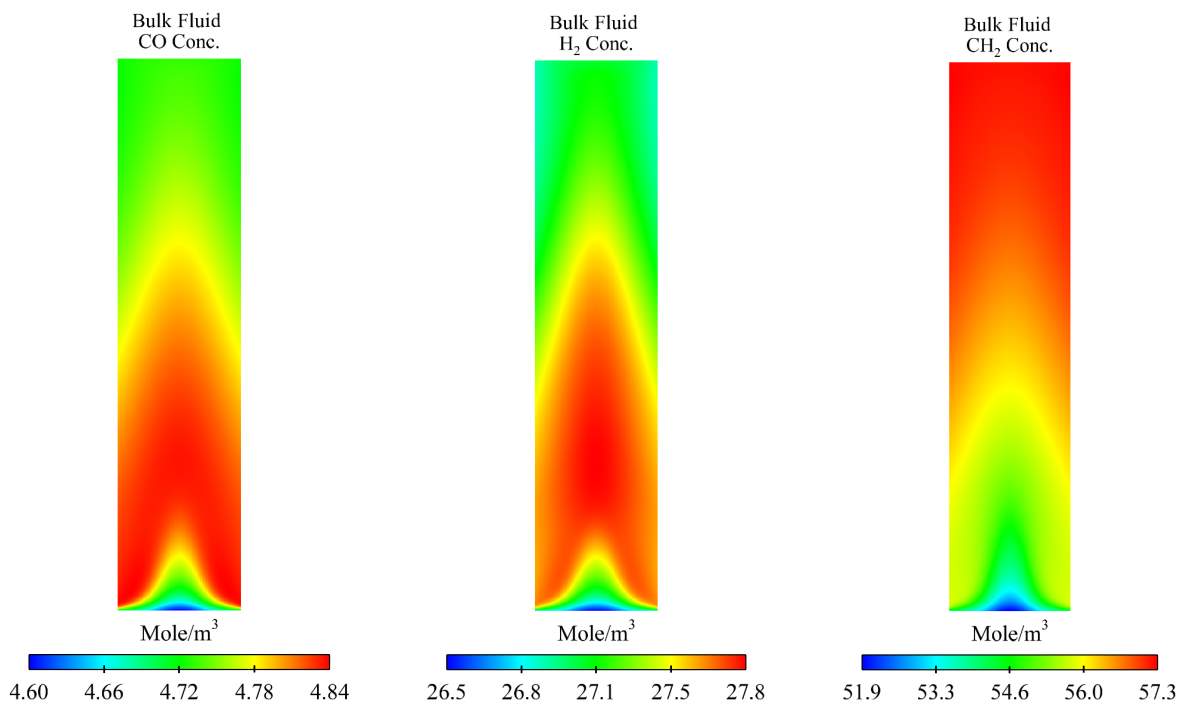


Figure 4. CO, H<sub>2</sub> and [-(CH<sub>2</sub>-)] concentration.

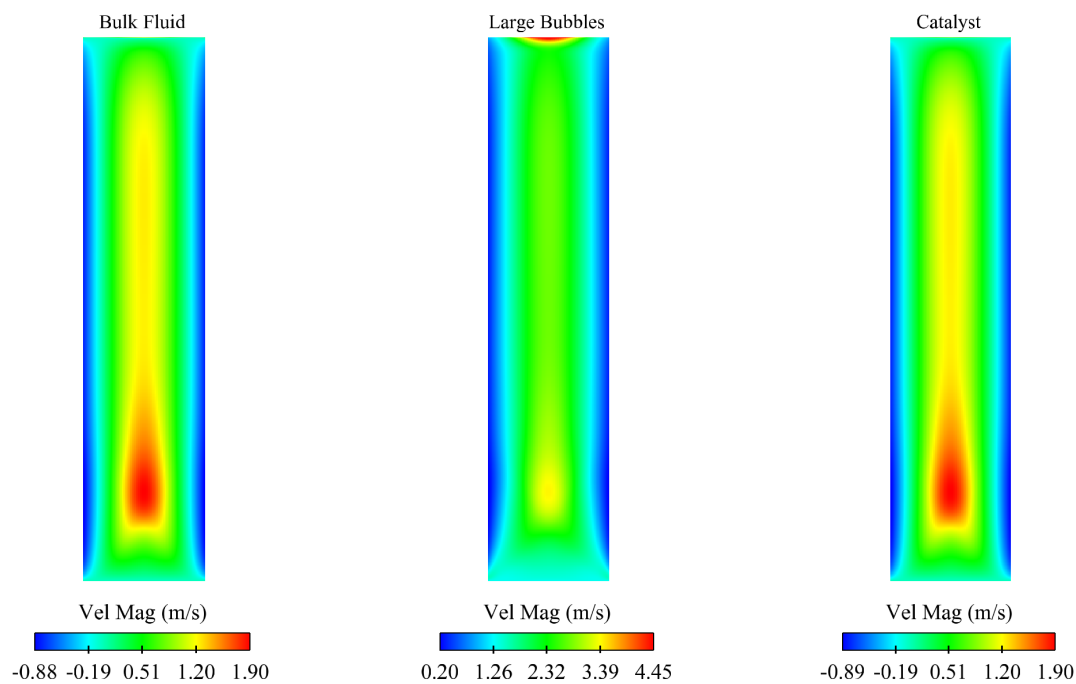


Figure 5. Velocity magnitude of bulk liquid, large bubbles and catalyst.

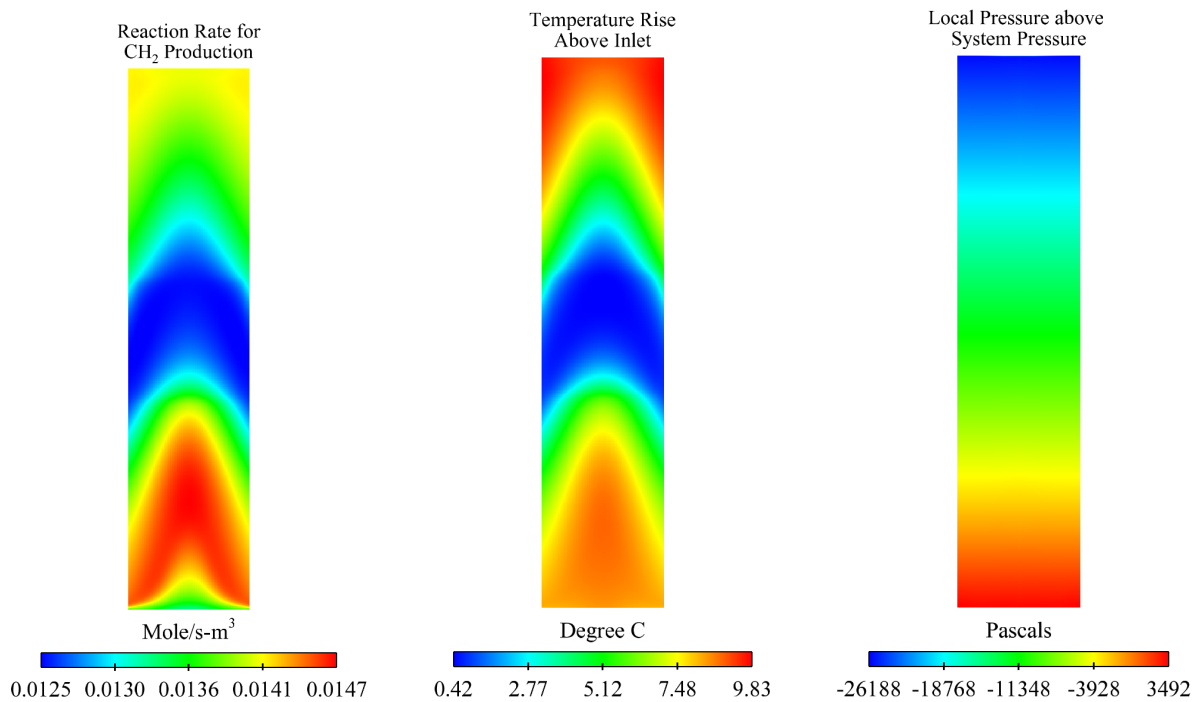


Figure 6. Reaction rate for  $[-(CH_2)-]$  production, temperature rise above inlet temperature and static pressure.

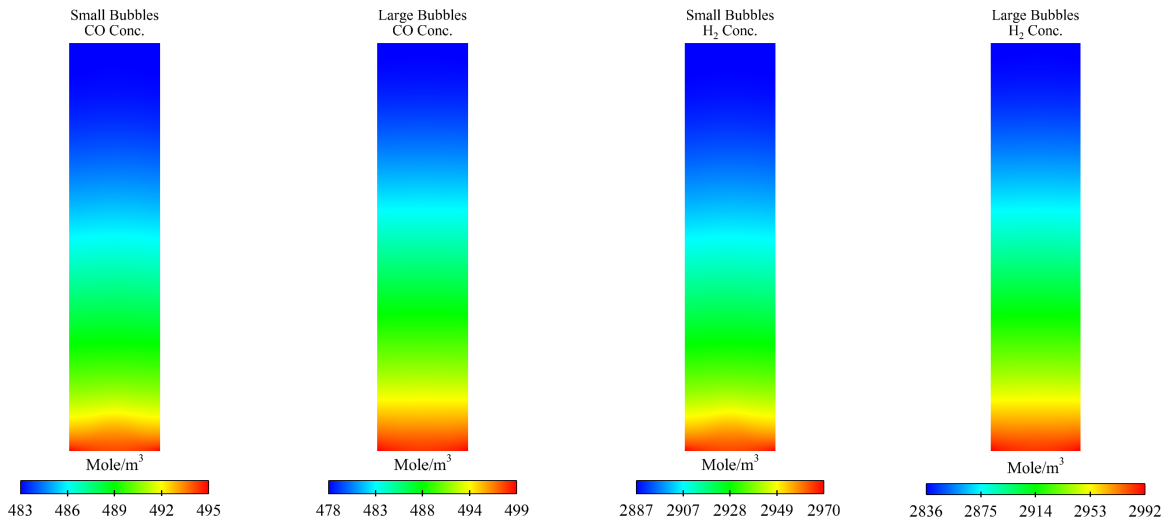


Figure 7. Small bubble CO concentration, large bubble CO concentration, small bubble H<sub>2</sub> concentration and large bubble H<sub>2</sub> concentration.

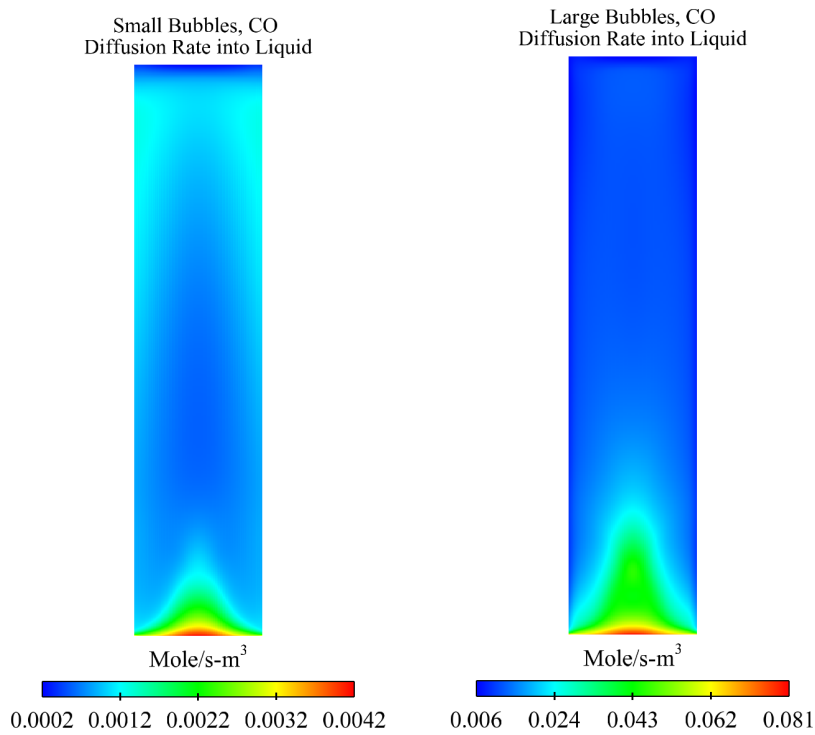


Figure 8. Diffusion rate of CO from small and large bubbles into liquid.

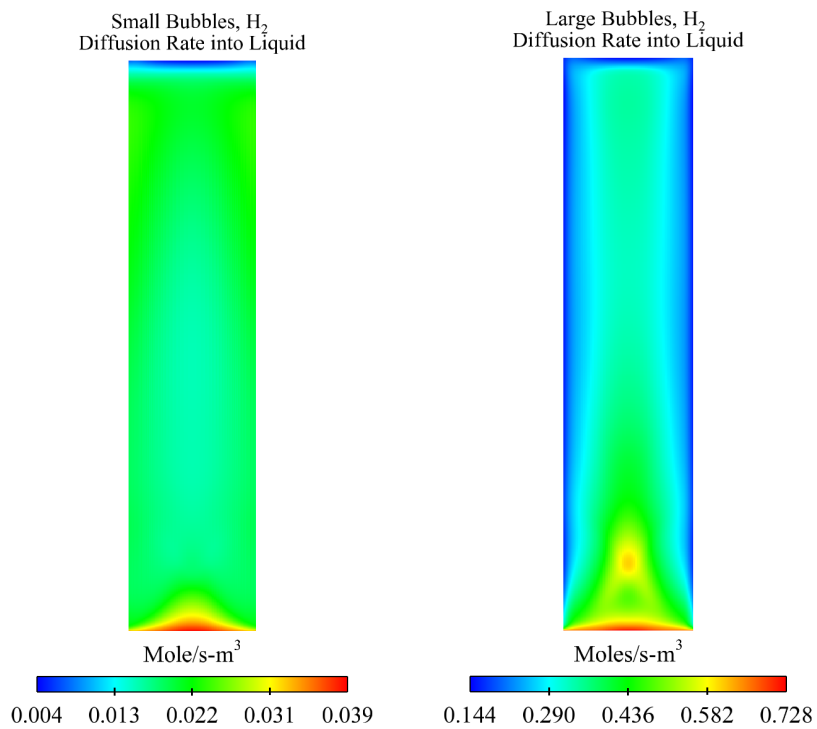


Figure 9. Small and large bubble H<sub>2</sub> diffusion rate into liquid.

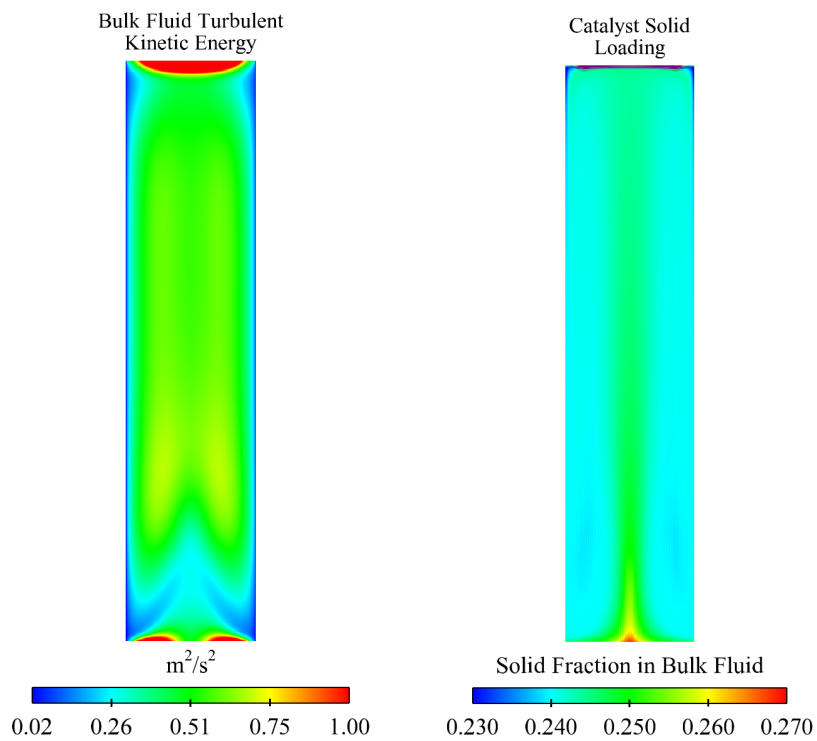


Figure 10. Bulk fluid turbulent kinetic energy and catalyst loading.